IEEE PEDS 2001 - INDONESIA

Sensitivity Analysis of Injection–Based Position Estimation in PM Synchronous Motors

Vladan Petrović, Aleksandar M. Stanković, and Miguel Vélez–Reyes

Abstract— **This paper analyzes effects of injection frequency selection on performance of position–sensorless algorithms for permanent magnet synchronous motors (PMSMs). The sensitivity with respect to the rotor position of the transfer function between the injected quantity (e.g. voltage) and its response (e.g. current) is explored over a wide frequency range. The paper then presents analytical results that optimize the selection of injection frequency in terms of motor and drive parameters. The frequency selection procedure is based on motor parameters that were obtained experimentally.**

Keywords— **Permanent magnet machines, position estimation, sensitivity analysis, motor drives.**

I. Introduction

Dominant techniques for achieving sensorless operation of PMSMs at low speeds are based on sinusoidal signal injection [1],[2],[3]. Existing guidelines for selection of the injection frequency, however, are only *qualitative*: 1)the selected frequency should be far enough from the DC so that there is no interference with signals corresponding to the basic energy conversion; 2) if the injected signals are currents, then injection frequency should be within the bandwidth of the current regulator.

The main aim of this paper is to provide a *quantitative* solution that would enable the design engineer to optimize the selected frequency depending on motor and drive parameters. Our main tool is the analysis of sensitivity of the transfer function between the injected signal and its response with respect to position for various injection frequencies. The analysis is performed in a wide injection frequency range, taking into account high frequency parasitic phenomena that modify motor behavior modeled with the standard PMSM model. Experimental data are used to confirm the validity of the motor model. Our results not only explain phenomena observed in the implementation of the injection-based sensorless control of PMSM, but also provide practical guidelines for designs of such schemes in terms of particular motor and drive parameters.

V. Petrović and A. M. Stanković are with the Department of Electrical and Computer Engineering, Northeastern University, 442 Dana Building, Boston, MA 02115, U.S.A. (email: {vpetrovi, astankov}@ece.neu.edu)

M. Vélez–Reyes is with the Electrical and Computer Engineering Department, University of Puerto Rico at Mayaguez, P.O. Box 9042, Mayaguez, PR 00681-9042, Puerto Rico - U.S.A. (email: mvelez@ece.uprm.edu)

V. Petrović and A. M. Stanković were supported by the U.S. National Science Foundation under grants ECS-9502636 and ECS-9820977, and by the U.S. Office of Naval Research under grant N14-95-1-0723. M. Vélez–Reyes was supported by the U.S. National Science Foundation under award ECS-9702860.

II. System Model and Estimation Approach

An example of estimation algorithm outlined in this paper is set into $\alpha\beta$ frame, as in this frame inductance matrix is position dependent. Namely, the electrical subsystem of a PM synchronous motor can be modeled as follows:

$$\mathbf{v} = \mathbf{R}\mathbf{i} + \mathbf{L}\frac{d\mathbf{i}}{dt} + \omega\frac{d\lambda_r}{d\theta} \tag{1}$$

where $\mathbf{x} = [x_\alpha,\ x_\beta]^\top$, $x \in \{v,\ i,\ \lambda_r\}$, and

$$\mathbf{L} = \begin{bmatrix} L_0 + L_1\cos(2\theta) & L_1\sin(2\theta) \\ L_1\sin(2\theta) & L_0 - L_1\cos(2\theta) \end{bmatrix},$$

$$\mathbf{R} = \begin{bmatrix} R_s - 2\omega L_1\sin(2\theta) & 2\omega L_1\cos(2\theta) \\ 2\omega L_1\cos(2\theta) & R_s + 2\omega L_1\sin(2\theta) \end{bmatrix}$$

This system is then excited with a periodic waveform in voltage $\mathbf{v}$ and the frequency response of the system is examined. Periodic waveform has a certain (relatively high) fundamental frequency, and no frequency content around DC in order to separate injection signal from the normal motor operation excitation (which has frequency content around frequency of the rotor rotation). We will assume in this analysis that mechanical variables (θ and ω) change negligibly over one period of injection waveform. Thus, the term $\omega\frac{d\lambda_r}{d\theta}$ is constant, and so are the parameters of resistance and inductance matrices. Another assumption will be that motor speed is low enough so that the terms in $\mathbf{R}$ matrix involving ω can be neglected (this assumption is reasonable, since injection based sensorless algorithms are usually used in the lower motor speed range). With these assumptions, $\omega\frac{d\lambda_r}{d\theta}$ has only a DC component, and $\mathbf{R} = diag\{R_s,\ R_s\}$. Using the notation $X = \frac{1}{T_i}\int_0^{T_i}\mathbf{x}(t)e^{-j\omega_i t}dt = X_c - jX_s$ for the fundamental injection frequency harmonic of a signal vector $\mathbf{x}$, from (1) follows

$$V_c - jV_s = R_sI_c - jR_sI_s + \mathbf{L}j\omega_iI_c + \mathbf{L}\omega_iI_s \Leftrightarrow$$

$$\begin{aligned} V_c &= R_sI_c + \mathbf{L}(\theta)\omega_iI_s \\ V_s &= R_sI_s - \mathbf{L}(\theta)\omega_iI_c \end{aligned} \tag{2}$$

which is a system of four real equations from which four unknowns R_s, L_0, L_1, and θ can be found. The details on the system solution and input selection will be given in Section V.

Besides the requirement that the injection signal should have a relatively high frequency to be separate from the normal excitation and not to affect the mechanical variables, no other specifications on auxiliary signal exist. In the following analysis, we will examine the effect of the injection frequency selection on the position estimation performance. This analysis is valid for any periodic injection

0-7803-7233-6/01/$10.00 ©2001 IEEE.

signal, although in many implementations the auxiliary signal is a simple sinusoid.

III. Sensitivity Analysis

The methodology used in this study is based on local methods for sensitivity analysis [4] using the sensitivity function. In sinusoidal injection–based position estimation the only control parameter of the input signal is its frequency, therefore for high parameter identifiability using this method, we want to select an input frequency where the sensitivity with respect to θ is high. In this way, the system output will be the most informative about the parameter of interest.

Let us denote the system transfer function with $\mathbf{T}(s,\theta)$. The definition of sensitivity is derived from the Taylor series of this function around some $\theta = \theta_0$:

$$\mathbf{T}(s,\theta) = \mathbf{T}(s,\theta_0) + \left.\frac{\partial \mathbf{T}(s,\theta)}{\partial\theta}\right|_{\theta=\theta_0} (\theta-\theta_0) + H.O.T. \Rightarrow$$

$$\|\mathbf{T}(s,\theta) - \mathbf{T}(s,\theta_0)\| \approx \left\| \left.\frac{\partial \mathbf{T}(s,\theta)}{\partial\theta}\right|_{\theta=\theta_0} \right\| |\theta-\theta_0| \Rightarrow$$

$$\frac{\|\mathbf{T}(s,\theta)-\mathbf{T}(s,\theta_0)\|}{\|\mathbf{T}(s,\theta_0)\|} \approx \frac{|\theta_0|}{\|\mathbf{T}(s,\theta_0)\|} \left\| \left.\frac{\partial \mathbf{T}(s,\theta)}{\partial\theta}\right|_{\theta=\theta_0} \right\| \frac{|\theta-\theta_0|}{|\theta_0|}$$

The term on the left is the relative change of the transfer function, the term $\frac{|\theta-\theta_0|}{|\theta_0|}$ is the relative change of θ, and the remaining term is the sensitivity:

$$S_\theta^{\mathbf{T}} = \frac{|\theta_0|}{\|\mathbf{T}(s,\theta_0)\|} \left\| \left.\frac{\partial \mathbf{T}(s,\theta)}{\partial\theta}\right|_{\theta=\theta_0} \right\| \tag{3}$$

At $s = j\omega$, this function gives information of the sensitivity of the system transfer function to position θ as a function of input signal frequency.

Since the motor is usually voltage supplied (particularly in the case when voltage source inverter is used), the transfer function matrix of interest is $\mathbf{T}(s,\theta) = (\mathbf{R}+\mathbf{L}s)^{-1}$. For derivation we first need explicit expression for this transfer function matrix:

$$\mathbf{T}(s,\theta) = \begin{bmatrix} \frac{R_s+sL_0-sL_1\cos(2\theta)}{(R_s+sL_0)^2-s^2L_1^2} & \frac{-sL_1\sin(2\theta)}{(R_s+sL_0)^2-s^2L_1^2} \\ \frac{-sL_1\sin(2\theta)}{(R_s+sL_0)^2-s^2L_1^2} & \frac{R_s+sL_0+sL_1\cos(2\theta)}{(R_s+sL_0)^2-s^2L_1^2} \end{bmatrix}$$

Further, we need the partial derivative of this function with respect to θ:

$$\frac{\partial \mathbf{T}(s,\theta)}{\partial\theta} = \frac{2sL_1}{(R_s+sL_0)^2-s^2L_1^2} \begin{bmatrix} \sin(2\theta) & -\cos(2\theta) \\ -\cos(2\theta) & -\sin(2\theta) \end{bmatrix}$$

The position dependent matrix above is orthonormal, implying that both its singular values are equal to 1. Thus the 2–norm of this matrix is unity, and the norm of the whole partial derivative matrix is

$$\left\| \frac{\partial \mathbf{T}(s,\theta)}{\partial\theta} \right\| = \left| \frac{2sL_1}{(R_s+sL_0)^2-s^2L_1^2} \right|, \quad \forall\theta\in\mathcal{R}, \forall s\in\mathcal{C} \tag{4}$$

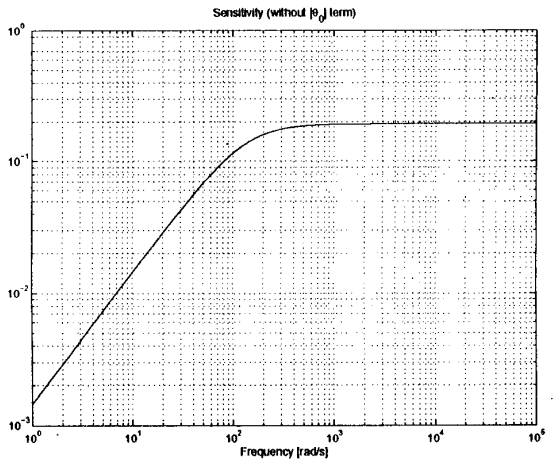

Fig. 1. Frequency dependence of the sensitivity function for the low frequency PMSM model with parameters $R_s = 1.25\Omega$, $L_0 = 8.4mH$, and $L_1 = -0.9mH$.

Notice that this norm is the same *for all* θ.

For completion of sensitivity calculation, we need norm, and thus singular values, of the transfer function itself. Singular values of $\mathbf{T}(s,\theta)$ are equal to the eigenvalues of $\mathbf{T}^*(s,\theta)\mathbf{T}(s,\theta)$, where $(\cdot)^*$ represents complex conjugate transpose. To this end, notice that $\mathbf{T}(s,\theta)$ can be rewritten as

$$\mathbf{T}(s,\theta) = T_1 \begin{bmatrix} 1 & 0 \\ 0 & 1 \end{bmatrix} + T_2 \begin{bmatrix} -\cos(2\theta) & -\sin(2\theta) \\ -\sin(2\theta) & \cos(2\theta) \end{bmatrix} \tag{5}$$

where $T_1 = \frac{R_s+sL_0}{(R_s+sL_0)^2-s^2L_1^2}$ and $T_2 = \frac{sL_1}{(R_s+sL_0)^2-s^2L_1^2}$. With such notation we have

$$\mathbf{T}^*(s,\theta)\mathbf{T}(s,\theta) = c_1 \begin{bmatrix} 1 & 0 \\ 0 & 1 \end{bmatrix} + c_2 \begin{bmatrix} -\cos(2\theta) & -\sin(2\theta) \\ -\sin(2\theta) & \cos(2\theta) \end{bmatrix}$$

where $c_1 = T_1^*T_1 + T_2^*T_2$ and $c_2 = T_1^*T_2 + T_1T_2^*$. Now, from $det(\mathbf{T}^*(s,\theta)\mathbf{T}(s,\theta) - \sigma^2\mathbf{I}) = 0$, it can be found that the singular values satisfy

$$(\sigma^2 - c_1)^2 - c_2^2 = 0 \Leftrightarrow \sigma_{1,2}^2 = c_1 \pm c_2 = |T_1 \pm T_2|^2$$

After the substitution of the expressions for T_1 and T_2, we get

$$\sigma_{1,2} = \left| \frac{R_s + sL_0 \pm sL_1}{(R_s+sL_0)^2 - s^2L_1^2} \right|$$

Finally, the largest of those two singular values is the norm of $\mathbf{T}(s,\theta)$, yielding

$$\|\mathbf{T}(s,\theta)\| = \left| \frac{R_s + sL_0 + s|L_1|}{(R_s+sL_0)^2 - s^2L_1^2} \right|, \quad \forall\theta\in\mathcal{R}, \forall s\in\mathcal{C} \tag{6}$$

Substitution of (4) and (6) into (3) finally yields the expression for the sensitivity function as

$$S_\theta^{\mathbf{T}} = |\theta_0| \left| \frac{2sL_1}{R_s + s(L_0 + |L_1|)} \right|, \quad \forall\theta\in\mathcal{R}, \forall s\in\mathcal{C}$$

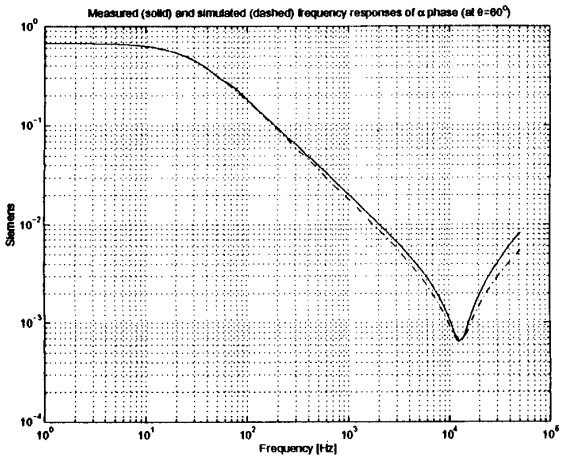

Fig. 2. Measured (solid) and model predicted (dashed) α phase admittance (at $\theta = 60°$) for model parameters $R_s = 1.25\Omega$, $L_0 = 8.4mH$, $L_1 = -0.9mH$, $C_p = 18nF$, and $G_p = 0.64mS$.

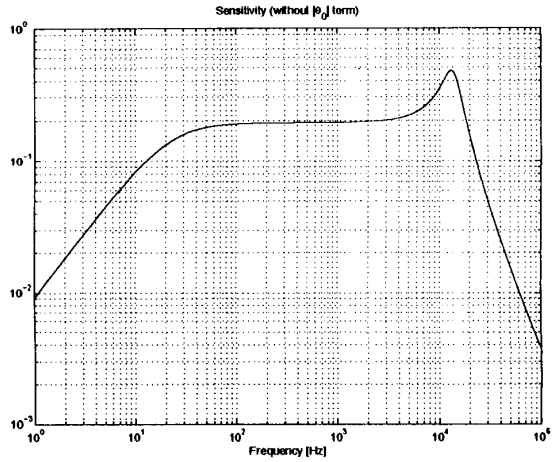

Fig. 3. Frequency dependence of the sensitivity function for the wide bandwidth PMSM model.

Without $|\theta_0|$ term, this function represents magnitude characteristic of a rational function, and its example is plotted in Fig. 1. This is a high–pass characteristic, so the sensitivity of the system transfer function with respect to θ is maximized for the frequencies higher than a cutoff frequency $\omega_{i_0} = \frac{R_s}{L_0+|L_1|}$.

Note: The exactly same result would be achieved from the analysis of a current supplied system whose transfer function is $\mathbf{T}(s,\theta) = \mathbf{R} + \mathbf{L}s$.

IV. High Frequency Parasitic Effects

The sensitivity analysis from the previous section yields valid results in the lower frequency regions (below about 10kHz) where the presented motor model is accurate. As the input signal frequency increases, however, the parasitic effects – parasitic capacitances, skin effect, hysteresis and eddy current losses – modify the low frequency system behavior and thus have to be included into the model. Several papers, including [5] and [6], address high frequency modeling of AC motors. Modeling of an AC motor at high frequencies is a very challenging problem, since at those frequencies motor behaves as a distributed parameter system, and has frequency dependent parameters. Nevertheless, rather accurate motor models with constant lumped parameters can be successfully fitted to the experimental data. In addition to the standard low frequency model (presented in the previous section), the resulting models, transformed into $\alpha\beta$ frame, include parallel capacitive and conductive components to account for the parasitic capacitances and additional motor losses.

In order to determine parameters of the wide bandwidth motor model, phase to phase impedance of a two–horsepower PM synchronous motor (model R43H, made by Pacific Scientific) was measured using HP35665A dynamic signal analyzer, and $\alpha\beta$ parameters were calculated to fit the experimental data. The parameters found from those measurements are $R_s = 1.25\Omega$, $L_0 = 8.4mH$, $L_1 = -0.9mH$, $C_p = 18nF$ (parasitic capacitance), and $G_p = 0.64mS$ (parallel conductance). Fig. 2 shows good matching of experimentally determined and model predicted α phase admittances.

Having acquired parameters, the complete model can be used in the sensitivity analysis. The transfer function that needs to be considered now becomes

$$\mathbf{T}_{hf}(s,\theta) = (\mathbf{R} + \mathbf{L}s)^{-1} + s\mathbf{C} + \mathbf{G}$$

where $\mathbf{C} = diag\{C_p,\ C_p\}$ is the matrix of parasitic capacitances and $\mathbf{G} = diag\{G_p,\ G_p\}$ is the matrix of conductances modeling additional motor losses. Note that this transfer function can also be rewritten in the form (5), with $T_1 = \frac{R_s+sL_0}{(R_s+sL_0)^2-s^2L_1^2} + sC_p + G_p$ and T_2 as before, and the similar analysis follows yielding

$$\|\mathbf{T}_{hf}(s,\theta)\| = \left|\frac{R_s+s(L_0+|L_1|)+(sC_p+G_p)((R_s+sL_0)^2-s^2L_1^2)}{(R_s+sL_0)^2-s^2L_1^2}\right|$$

for all θ. Since (4) remains valid in this case as well, the sensitivity of the wide bandwidth transfer function with respect to the rotor position is finally given with

$$S_\theta^{\mathbf{T}_{hf}} = |\theta_0|\left|\frac{2sL_1}{R_s+s(L_0+|L_1|)+(sC_p+G_p)((R_s+sL_0)^2-s^2L_1^2)}\right|$$

for all θ. The frequency dependence of this function, without $|\theta_0|$ term, is shown in Fig. 3. As can be seen from the plot, the sensitivity function in this case has a more realistic, band–pass characteristic. As in the previous case, at very low frequencies motor resistance dominates position dependent inductance and the sensitivity is low. With the increase in injection frequency, the sensitivity increases up to a cutoff frequency ω_{i_0}, after which it stagnates. However, at much higher frequencies, parasitic capacitances

start dominating, and sensitivity decreases with increase in the injection frequency.

Based on the above sensitivity analysis, we conclude that the injection–based position–sensorless algorithm performs the best for a selection of the injection frequency between the cutoff frequency ω_{i_0} and the resonant frequency of the motor inductance and the parasitic capacitances. The simulations showing the advantages of a proper injection frequency selection will be presented in the following section.

V. Simulation Results

As described in Section II, the harmonic analysis of the electrical subsystem at the injection frequency yields the system (2) which can be developed as

$$\begin{aligned} V_{c_\alpha} &= R_s I_{c_\alpha} + \omega_i (L_0 + L_1 \cos(2\theta)) I_{s_\alpha} + \omega_i L_1 \sin(2\theta) I_{s_\beta} \\ V_{c_\beta} &= R_s I_{c_\beta} + \omega_i L_1 \sin(2\theta) I_{s_\alpha} + \omega_i (L_0 - L_1 \cos(2\theta)) I_{s_\beta} \\ V_{s_\alpha} &= R_s I_{s_\alpha} - \omega_i (L_0 + L_1 \cos(2\theta)) I_{c_\alpha} - \omega_i L_1 \sin(2\theta) I_{c_\beta} \\ V_{s_\beta} &= R_s I_{s_\beta} - \omega_i L_1 \sin(2\theta) I_{c_\alpha} - \omega_i (L_0 - L_1 \cos(2\theta)) I_{c_\beta} \end{aligned}$$

and written in terms of the unknown parameter vector $\mathbf{p_i}$ as

$$\underbrace{\begin{bmatrix} V_{c_\alpha} \\ V_{c_\beta} \\ V_{s_\alpha} \\ V_{s_\beta} \end{bmatrix}}_{\mathbf{b}} = \underbrace{\begin{bmatrix} \omega_i I_{s_\alpha} & \omega_i I_{s_\alpha} & \omega_i I_{s_\beta} & I_{c_\alpha} \\ \omega_i I_{s_\beta} & -\omega_i I_{s_\beta} & \omega_i I_{s_\alpha} & I_{c_\beta} \\ -\omega_i I_{c_\alpha} & -\omega_i I_{c_\alpha} & -\omega_i I_{c_\beta} & I_{s_\alpha} \\ -\omega_i I_{c_\beta} & \omega_i I_{c_\beta} & -\omega_i I_{c_\alpha} & I_{s_\beta} \end{bmatrix}}_{\mathbf{A}} \underbrace{\begin{bmatrix} L_0 \\ L_1 \cos(2\theta) \\ L_1 \sin(2\theta) \\ R_s \end{bmatrix}}_{\mathbf{p_i}} \quad (7)$$

To be able to solve this system, matrix A has to be non–singular, and one of the input selections that satisfies this requirement is:

$$\mathbf{v}(t) = \begin{bmatrix} V_i \cos(\omega_i t) \\ \pm V_i \sin(\omega_i t) \end{bmatrix} \Rightarrow V = \frac{1}{2} \begin{bmatrix} V_i \\ \mp j V_i \end{bmatrix} \quad (8)$$

where V_i is the injection signal magnitude. With such motor excitation, the measured current response is used to calculate the current harmonics, and the motor parameter vector $\mathbf{p_i}$ are determined as the solution of the system (7). The rotor position is finally found from this vector using the inverse trigonometric functions.

To support the analytical results developed in the previous sections, the presented position estimation scheme was tested in simulations. The PMSM model (1) was excited with the injection waveform (8) having different frequencies and magnitudes. The motor electrical parameters are chosen as before: $R_s = 1.25\Omega$, $L_0 = 8.4mH$, and $L_1 = -0.9mH$, and the injection magnitude was selected such that for each signal frequency the injected current has the magnitude of $I_i = 0.37A$ (which corresponds to 3.8% of the R43H motor rated current). To model the measurement and quantization noise existing in practical implementations, current measurements were corrupted with a white Gaussian noise with mean $\mu = 24mA$ and variance $\sigma^2 = 40 \cdot 10^{-6} A^2$.

The simulations described above were used to evaluate the performance of the position estimation algorithm for several values of the injection frequency. The resulting position estimation errors for frequencies $f_i = 0.1$, 1, 10, and $100Hz$ are shown in Fig. 4, and the corresponding position estimate noise variances are found to be $\sigma_e^2 = 0.397$, $4.05 \cdot 10^{-3}$, $4.85 \cdot 10^{-5}$, and $7.53 \cdot 10^{-6}$, respectively. As these results show, the accuracy of the position estimation increases by an order of magnitude with each tenfold increase of the injection frequency up to the cutoff frequency ($\omega_{i_0} = 134.4 rad/s \Rightarrow f_{i_o} = 21.4Hz$ for the experimentally determined motor parameters), and after ω_{i_0} the accuracy stagnates. Thus, the simulations support the conclusions drawn in the previous sections since exactly the same results were predicted by the sensitivity analysis (refer to Fig. 1).

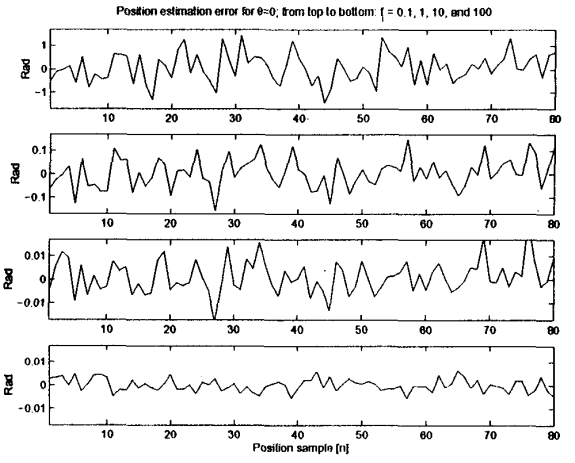

Fig. 4. Position estimation errors for different injection signal frequencies.

VI. Conclusions

This paper addressed the selection of the input signal frequency selection in injection–based position estimation in permanent magnet synchronous motors with magnetic saliency. The main idea behind our analysis is that the test signal frequency in injection–based algorithms should be selected to achieve a high output sensitivity to the change in position in order to ensure reliable estimation in the presence of noise. The sensitivity analysis provided guidelines for injection signal frequency selection which explain and support the common choices in the current practice. The results suggest that the test signal frequency should be selected as high as possible, up to the limit set by the motor parasitic effects. The validity of those results was also confirmed by numerical simulations of an injection–based position estimation algorithm.

References

[1] M. J. Corley and R. D. Lorenz, "Rotor position and velocity estimation for a salient–pole permanent magnet synchronous machine at standstill and high speeds," *IEEE Transactions on Industry Applications*, vol. 34, no. 4, pp. 784–789, 1998.

[2] J.–M. Kim, S.–J. Kang, and S.–K. Sul, " Vector control of interior permanent magnet synchronous motor without shaft sensor," *Conf. Proc. IEEE APEC*, vol. 2, Atlanta, GA, Feb. 1997, pp. 743–748.

[3] T. Aihara, A. Toba, T. Yanase, A. Mashimo, K. Endo, "Sensorless torque control of salient-pole synchronous motor at zero-speed operation," *IEEE Transactions on Power Electronics*, vol. 14, no. 1, pp. 202–208, 1999.
[4] A. Saltelli, K. Chan, E.M. Scott, editors, *Sensitivity Analysis*, John Wiley, 2000.
[5] A. Boglietti and E. Carpaneto, "Induction motor high frequency model," *Conf. Rec. IEEE IAS Annual Meeting*, vol. 3, Phoenix, AZ, Oct. 1999, pp. 1551–1558.
[6] S. D. Sudhoff, J. L. Tichenor, and J. L. Drewniak, "Wide-Bandwidth multi-resolutional analysis of a surface-mounted PM synchronous machine," *IEEE Transactions on Energy Conversion*, vol. 14, no. 4, pp. 1011–1018, 1999.